Acta Cryst E CRYSTALLOGRAPHIC COMMUNICATIONS

ISSN 2056-9890

Crystal structure and Hirshfeld surface analysis of 6-bromo-2-(pentafluorophenyl)-2,3,7,7a-tetrahydro-3a,6-epoxyisoindol-1(6*H*)-one

Viktoria S. Maslova,[a] Veronika M. Cherepanova,[a] Victor N. Khrustalev,[a,b] Mehmet Akkurt,[c] Gizachew Mulugeta Manahelohe,[d]* Khudayar I. Hasanov[e] and Narmina A. Guliyeva[f]

[a]RUDN University, 6 Miklukho-Maklaya St., Moscow 117198, Russian Federation, [b]Zelinsky Institute of Organic Chemistry of RAS, Leninsky Prospect 47, Moscow 119991, Russian Federation, [c]Department of Physics, Faculty of Sciences, Erciyes University, 38039 Kayseri, Türkiye, [d]Department of Chemistry, University of Gondar, PO Box 196, Gondar, Ethiopia, [e]Azerbaijan Medical University, Scientific Research Centre (SRC), A. Kasumzade St. 14, AZ 1022, Baku, Azerbaijan, and [f]Department of Chemical Engineering, Baku Engineering University, Hasan Aliyev str. 120, AZ0101, Khirdalan, Absheron, Azerbaijan. *Correspondence e-mail: Gizachew.Mulugeta@uog.edu.et

Received 24 July 2026
Accepted 6 August 2026

Edited by B. Therrien, University of Neuchâtel, Switzerland

Keywords: enantiomeric crystal; pentafluorophenyl ring; pyrrolidine ring; hydrogen bond; Hirshfeld surface analysis.

CCDC reference: 2579217

Supporting information: this article has supporting information at journals.iucr.org/e

In the crystal, enantiomeric molecules of $C_{14}H_7BrF_5NO_2$ are linked by C—H···O hydrogen bonds, forming layers parallel to the $(\bar{1}01)$ plane. In addition, C—H···π interactions and Br···π contacts create layers parallel to the $(10\bar{1})$ plane. According to Hirshfeld surface analysis, the most important contributions to the crystal packing are F···H / H···F (32.4%), O···H / H···O (12.4%), F···F (11.5%), Br···F / F···Br (8.4%) and C···H / H···C (8.4%) interactions.

1. Chemical context

Fluorinated organic compounds occupy a special place among functionally substituted molecules, since the introduction of fluorine atoms significantly affects the electronic structure and polarity of molecules (Reichenbächer *et al.*, 2005; Cole & Taylor, 2022). In this regard, polyfluorinated aromatic systems containing halogen atoms capable of acting as a halogen-bond donor are of particular interest. According to modern concepts, a halogen bond occurs when an electrophilic region associated with a halogen atom interacts with the nucleophilic centre of another molecule or the same molecule (Desiraju *et al.*, 2013; Huseynov *et al.*, 2021). The directionality of such a bond is usually explained by the presence of a σ-hole region of positive electrostatic potential on the continuation of the C—*X* bond (Politzer *et al.*, 2010; Maslova *et al.*, 2026). Polyfluorination of the aromatic fragment enhances the electron-acceptor character of the system and can increase the positive potential on the halogen atom, thereby increasing the ability of the compound to form halogen bonds (Riley *et al.*, 2011; Mamedov *et al.*, 2024; Javadzade *et al.*, 2026). Although bromine-containing donors usually form weaker interactions compared to iodine-containing analogues, the presence of a pentafluorophenyl fragment makes such systems promising candidates for studying Br···N, Br···O, and Br···π contacts (Yang *et al.*, 2018; Guseinov *et al.*, 2025; Makhmudova *et al.*, 2022). We therefore synthesized and elucidated the crystal structure of the title compound.

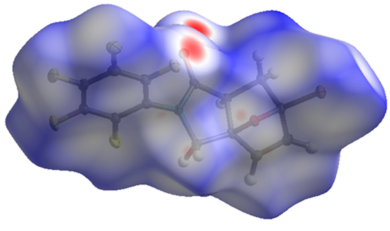

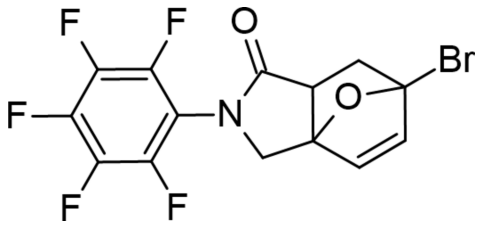

2. Structural commentary

The title compound crystallizes in the centrosymmetric space group $P2_1/n$, and therefore occurs as a racemic mixture of the 3a*R*,6*S*,7a*S* and 3a*S*,6*R*,7a*R* enantiomers. In the seven-membered ring system (O8/C3*A*/C4–C7/C7*A*) of the molecule (Fig. 1), the two five-membered *A* and *B* rings (*A*: O8/C3A/C4–C6 and *B*: O8/C3*A*/C6/C7/C7*A*) have the puckering parameters $Q(2)$ = 0.6054 (19) Å, $\varphi(2)$ = 355.9 (2)°, and $Q(2)$ = 0.267 (2) Å, $\varphi(2)$ = 282.7 (4)°, respectively, and adopt an envelope conformation on the O8 atom. The six-membered ring (*C*: C3*A*/C4–C7/C7*A*) has the puckering parameters Q_T = 0.947 (2) Å, θ = 90.74 (12)°, φ = 177.46 (13)° and exhibits a boat conformation. The five-membered pyrrolidine ring (*D*: N2/C1/C3/C3A/C7*A*) fused to the seven-membered ring system (O8/C3*A*/C4–C7/C7*A*) has the puckering parameters $Q(2)$ = 0.267 (2) Å, $\varphi(2)$ = 282.7 (4) ° and adopts an envelope conformation on atom C3*A*. The angles between the pentafluorophenyl ring (*E*: C8–C13) and the *C* (C3*A*/C4–C7/C7*A*) and *D* (N2/C1/C3/C3*A*/C7*A*) planes are 45.95 (11) and 69.23 (10)°, respectively. The *C* and *D* rings subtend an angle of 39.15 (12)°. The bond lengths and angles are comparable to those in the related structures discussed in the *Database survey* section.

3. Supramolecular features and Hirshfeld surface analysis

In the crystal, molecules are linked by C—H···O hydrogen bonds, forming layers parallel to the ($\bar{1}$01) plane (Table 1, Fig. 2). In addition, C—H···π (Table 1) and Br···π interactions [(C6)Br1···*Cg*5^{ii}: C6—Br1 = 1.9249 (18) Å, Br1···*Cg*5^{ii} = 3.6147 (9) Å, C6···*Cg*5^{ii} = 3.988 (2) Å and C6—Br1···*Cg*5^{ii} = 86.43 (6)°; *Cg*5 is the centroid of the pentafluorophenyl ring (C8–C13); symmetry code (ii) $-x+1, -y+1, -z+1$] act in opposite directions of the plane of the pentafluorophenyl ring, bonding molecules form layers parallel to the (10$\bar{1}$) plane (Fig. 3).

In order to quantify the intermolecular interactions, a Hirshfeld surface analysis was carried out using *Crystal Explorer 21* (Spackman *et al.*, 2021) and the associated two-dimensional fingerprint plots were generated. The Hirshfeld

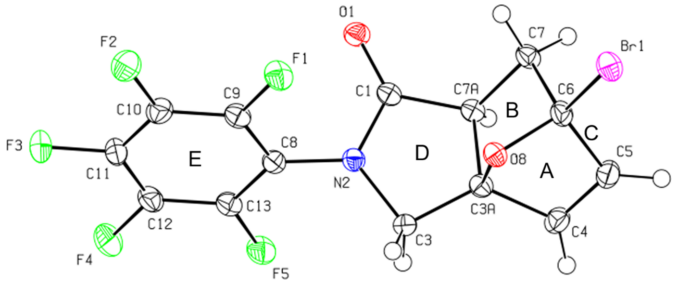

Figure 1
Molecular structure showing the atom labelling and ring system with displacement ellipsoids at 50% probability level.

Table 1
Hydrogen-bond geometry (Å, °).

*Cg*5 is the centroid of the pentafluorophenyl ring (C8–C13).

D—H···*A*	*D*—H	H···*A*	*D*···*A*	*D*—H···*A*
C3—H3*A*···O1^{i}	0.99	2.60	3.167 (2)	117
C3—H3*B*···O8^{ii}	0.99	2.60	3.410 (2)	140
C4—H4···O1^{iii}	0.95	2.38	3.309 (3)	167
C7*A*—H7*C*···O1^{i}	1.00	2.48	3.109 (3)	120
C7*A*—H7*C*···*Cg*5^{i}	1.00	2.87	3.790 (2)	153

Symmetry codes: (i) $-x+\frac{1}{2}, y-\frac{1}{2}, -z+\frac{1}{2}$; (ii) $-x+1, -y+1, -z+1$; (iii) $x, y-1, z$.

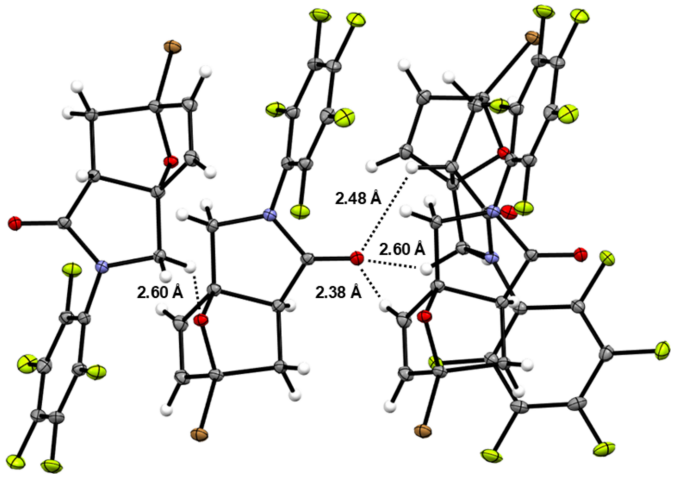

Figure 2
Partial packing view showing the C—H···O hydrogen bonds.

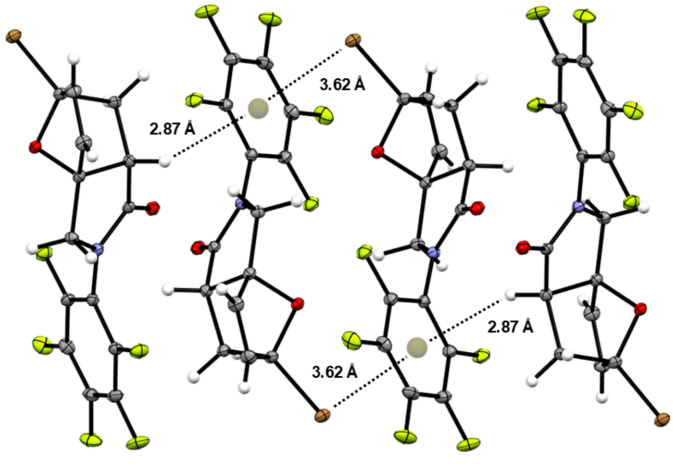

Figure 3
Partial packing view showing the C—H···π interactions and Br···π contacts with centroids of pentafluorophenyl rings.

Table 2
Summary of short interatomic contacts (Å).

Contact	Distance	Symmetry operation
Br1···H5	3.11	$\frac{3}{2}-x,\frac{1}{2}+y,\frac{1}{2}-z$
F1···F1	2.64	$1-x,2-y,1-z$
H3B···O8	2.60	$1-x,1-y,1-z$
H7B···F3	2.56	$\frac{1}{2}+x,\frac{3}{2}-y,-\frac{1}{2}+z$
O1···H4	2.38	$x,1+y,z$
F4···F3	2.97	$-x,2-y,1-z$
F4···F4	2.80	$-x,1-y,1-z$
H7C···O1	2.48	$\frac{1}{2}-x,-\frac{1}{2}+y,\frac{1}{2}-z$

surface mapped over d_{norm} in the range −0.2735 to +1.2893 a.u. is shown in Fig. 4, using colours to indicate contacts that are shorter (red areas), equal to (white areas), or longer than (blue areas) the sum of the van der Waals radii. The C—H···O interactions are indicated by red areas on the Hirshfeld surfaces (Tables 1 and 2).

The two-dimensional fingerprint plots provide quantitative information about the non-covalent interactions and the crystal packing in terms of the percentage contribution of the interatomic contacts. The overall two-dimensional fingerprint plot is shown in Fig. 5*a*. The dominant interactions in the crystal packing are F···H/H···F (32.4%), O···H/H···O (12.4%), F···F (11.5%), Br···F / F···Br (8.4%) and C···H/H···C (8.4%) contacts; see Fig. 5*b–f*. The other contacts (H···H 6.7%, Br···H/H···Br 5.9%, Br···C/C···Br 4.6%, O···C/C···O 2.5%, F···O/O···F 2.2%, F···C/C···F 1.7%, C···C 1.6%, Br···Br 1.2%, O···N/N···O 0.3% and N···H/H···N 0.1%) only make a minor contribution to the crystal packing.

4. Database survey

A search of the Cambridge Structural Database (CSD, Version 6.00, update of April 2025; Groom *et al.*, 2016) for the 1,2,3,6,7,7a-hexahydro-3a,6-epoxyisoindole unit revealed five analogues: BILLEP (Mitchell *et al.*, 2013), BILLAL (Mitchell *et al.*, 2013), VAMREL (Shchevnikov *et al.*, 2026), DUBYUX (Tan *et al.*, 2020) and DUBZAE (Tan *et al.*, 2020).

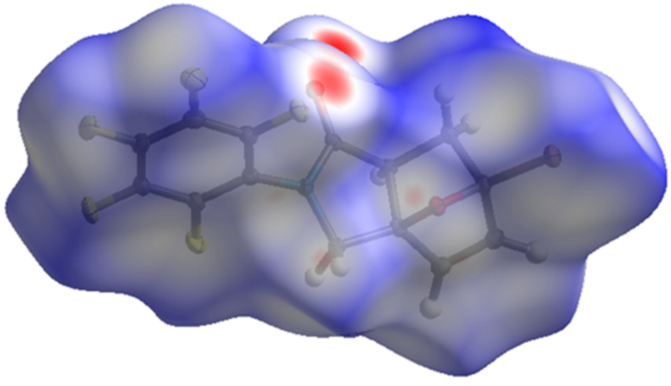

Figure 4
View of the three-dimensional Hirshfeld surface plotted over d_{norm} in the range −0.2735 to 1.2893 a.u.

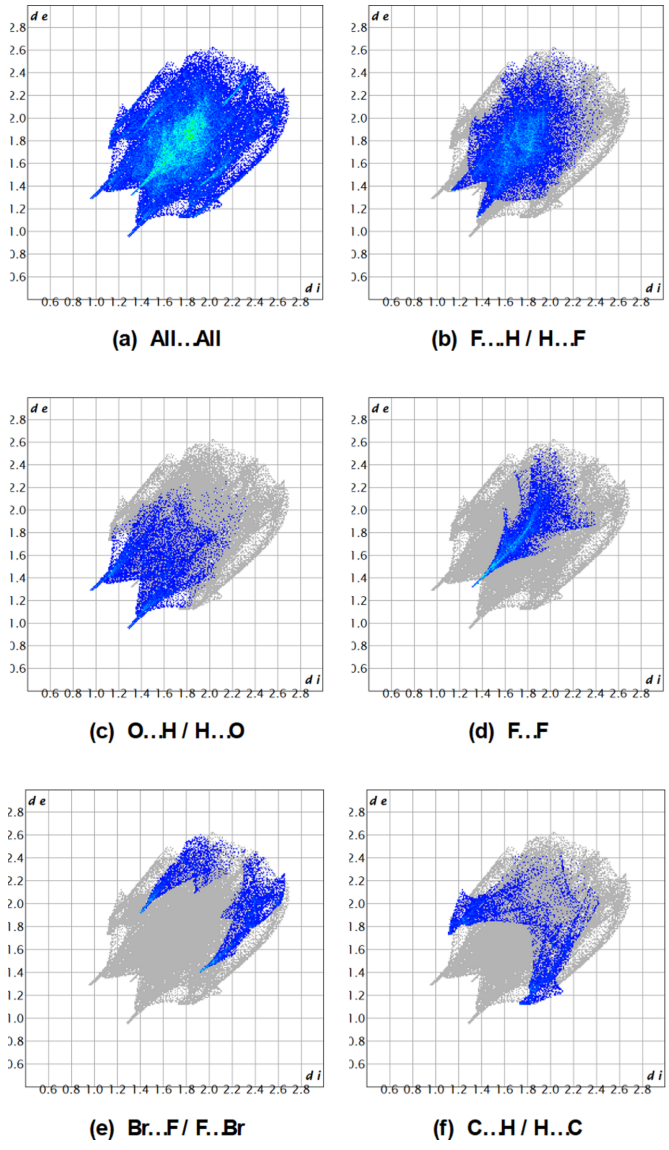

Figure 5
The two-dimensional fingerprint plots showing (*a*) all interactions, and those delineated into (*b*) F···H/H···F, (*c*) O···H/H···O, (*d*) F···F, (*e*) Br···F/F···Br and (*f*) C···H/H···C interactions. The d_i and d_e values are the closest internal and external distances (in Å) from given points on the Hirshfeld surface.

Although there are no conventional hydrogen bonds in BILLEP, there are weaker interactions between the molecules, such as C—H···O and C—H···N, as compared to N—H···O hydrogen bonds in BILLAL. Compound BILLAL packs head-to-head with hydrogen bonding, whereas compound BILLEP packs head-to-tail with regard to the ether groups.

The asymmetric unit of VAMREL contains two crystallographically independent molecules in which the cyclohexene and pyrrole rings are in boat and envelope conformations, respectively. In the crystal, C—H···O and N—H···Se hydrogen bonds link the molecules into [100] chains, enclosing $R_2^2(20)$, $R_3^3(18)$ and $R_4^4(4)$ ring motifs (Bernstein *et al.*, 1995). C—H···π (ring) interactions help to consolidate the packing.

In DUBYUX, molecules are linked by π–π interactions into chains along the *b*-axis direction. At the same time, C—H$\cdots\pi$ interactions also link DUBYUX molecules into chains extending along the *b*-axis direction. These interactions form layers parallel to the *ab* plane. In the crystal structure of DUBZAE, hydrogen bonds, C— H$\cdots\pi$ and π–π interactions occur between molecules.

5. Synthesis and crystallization

Pentafluoroaniline (1045 mg, 5.71 mmol) was added to the corresponding 5-bromofurfural (1000 mg, 5.71 mmol) in toluene (20 ml). The reaction mixture was heated under reflux for 5 days using a Dean–Stark trap (TLC control). After the reaction was completed, the solution was concentrated. The residue was dissolved in methanol (15 ml) and sodium borohydride (430 mg, 11.4 mmol) was added portionwise (36 mg in every 5 min) over a period of 1 h. The resulting mixture was stirred at room temperature for 24 h (TLC control, hexane–EtOAc, 10:1). The reaction mixture was poured into water (30 ml) and extracted with DCM (3 × 30 ml). The organic layers were dried with anhydrous $MgSO_4$, concentrated and purified by column chromatography (SiO_2, 23 × 1.6 cm, eluent hexane-EtOAc, 50:1) to afford *N*-[(5-bromofuran-2-yl)methyl]-2,3,4,5,6-pentafluoroaniline in good yield. Yellow oil, yield 63%, 1228 mg (3.59 mmol). ^{1}H NMR (700.2 MHz, $CDCl_3$), (*J*, Hz) δ 6.22 (*s*, 2 H, H-3 and H-4 Fur), 4.42 (*d*, *J* = 7.2 Hz, 2 H, NCH_2), 4.01 (*br. s*, 1 H, NH). ^{13}C NMR (176.1 MHz, $CDCl_3$) δ 153.8, 138.4 (*dm*, *J* = 244.4 Hz, 2 C, C—F), 138.1 (*dm, J* = 248.5 Hz, 2 C, C—F), 134.3 (*dm, J* = 245.8 Hz, 1 C, C—F), 122.5 (*t, J* = 12.1 Hz, 1 C, C—Ar), 121.9, 112.0, 110.7, 42.9 (*t, J* = 4.1 Hz, 1 C, CH_2). ^{19}F NMR (658.8 MHz, $CDCl_3$) δ −158.0 (*d, J* = 21.5 Hz, 2 F, F-2,6 Ar), −163.9 (*t, J* = 21.5 Hz, 2 F, F-3,5 Ar), −169.5 (*d, J* = 21.5 Hz, 1 F, F-4 Ar). IR (KBr, cm^{-1}): ν_{max} = 3316 (NH), 1124, 1011, 964, 787 (C-Hal). GC—MS (EI, 70 eV) *m*/*z*: 343 [*M*, Br^{81}]$^+$, 341 [*M*, Br^{79}]$^+$, 194 (10), 161 (98), 159 (100), 155 (14), 133 (45), 131 (47), 117 (13), 51 (26).

N-[(5-bromofuran-2-yl)methyl]-2,3,4,5,6-pentafluoroaniline (1200 mg, 3.51 mmol), and Et_3N (1.1 ml, 8.07 mmol) were dissolved in pseudocumene (50 ml) and stirred for 5 min. Acryloyl chloride was added (0.51 ml, 6.32 mmol), and the reaction mixture was heated under reflux for 5 days (TLC control, hexane–EtOAc, 1:1). After cooling, the reaction mixture was filtered, and the filtrate was poured into water (30 ml) and extracted with EtOAc (3 × 30 ml). The organic layers were dried with anhydrous $MgSO_4$. The solvent was evaporated at reduced pressure, and the residue was triturated with ether (2 × 15 ml) to isolate 6-bromo-2-(pentafluorophenyl)-2,3,7,7a-tetrahydro-3a,6-epoxyisoindol-1(6*H*)-one. The precipitate was filtered off and washed with ether (2 × 15 ml). Brown powder, yield 47%, 653 mg (1.65 mmol), m.p. 453–455 K. Single crystals were grown in DMSO at 281 K. ^{1}H NMR (700.2 MHz, $CDCl_3$), (*J*, Hz) δ 6.56 and 6.55 (two *d, J* = 5.7 Hz, 2 H, H-4 and H-5), 4.41 (*d, J* = 11.4 Hz, 1 H, H-3A), 4.08 (*d, J* = 11.4 Hz, 1 H, H-3B), 2.83 (*dd, J* = 8.6, 3.6 Hz, 1 H, H-7a), 2.66 (*dd, J* = 12.2, 3.6 Hz, 1 H, H-7A), 2.35 (*dd, J* = 12.2, 8.6 Hz, 1 H, H-7B). ^{13}C NMR (176.1 MHz, $CDCl_3$) δ 172.0, 144.1 (*dm, J* = 253.9 Hz, 2 C, C—F), 141.6, 141.2 (*dm, J* = 255.9 Hz, 1 C, C—F), 138.0 (*dm, J* = 247.8 Hz, 2 C, C—F), 133.6, 112.7 (*t, J* = 11.5 Hz, 1 C, C—Ar), 88.8, 88.5, 51.3, 49.4, 39.6. ^{19}F NMR (658.8 MHz, DMSO-d_6) δ −144.3 (*br. s*, 2 F, F-2,6 Ar), −155.5 (*d, J* = 21.5 Hz, 1 F, F-4 Ar), −162.8 (*t, J* = 21.5 Hz, 2 F, F-3,5 Ar). IR (KBr, cm^{-1}): ν_{max} = 1709 (C=O), 1120, 1095, 953, 926, 840, 718, 662 (C–Hal). GC—MS (EI, 70 eV) *m*/*z*: 397 [*M*, Br^{81}]$^+$, 395 [*M*, Br^{79}]$^+$, 316 (100), 220 (31), 194 (36), 167 (13), 161 (62), 159 (60), 132 (15), 131 (23), 117 (12), 77 (15), 55 (58).

Table 3
Experimental details.

Crystal data	
Chemical formula	$C_{14}H_7BrF_5NO_2$
M_r	396.11
Crystal system, space group	Monoclinic, $P2_1/n$
Temperature (K)	100
a, *b*, *c* (Å)	13.4425 (1), 7.0992 (1), 14.9829 (2)
β (°)	106.241 (1)
V (Å^3)	1372.77 (3)
Z	4
Radiation type	Cu *K*α
μ (mm^{-1})	4.76
Crystal size (mm)	0.45 × 0.33 × 0.20
Data collection	
Diffractometer	Rigaku XtaLAB Synergy-S, HyPix-6000HE area-detector
Absorption correction	Analytical [*CrysAlis PRO* (Agilent, 2014). Analytical numeric absorption correction using a multifaceted crystal model based on expressions derived by Clark & Reid (1995)]
T_{min}, T_{max}	0.385, 0.622
No. of measured, independent and observed [$I > 2\sigma(I)$] reflections	15639, 2965, 2814
R_{int}	0.041
(sin $\theta/\lambda)_{max}$ (Å^{-1})	0.638
Refinement	
$R[F^2 > 2\sigma(F^2)]$, $wR(F^2)$, *S*	0.033, 0.094, 1.08
No. of reflections	2965
No. of parameters	209
H-atom treatment	H-atom parameters constrained
$\Delta\rho_{max}$, $\Delta\rho_{min}$ (e Å^{-3})	0.56, −0.65

Computer programs: *CrysAlis PRO* (Agilent, 2014), *SHELXT* (Sheldrick, 2015*a*), *SHELXL* (Sheldrick, 2015*b*), *ORTEP-3 for Windows* (Farrugia, 2012), *Mercury* (Macrae *et al.*, 2020) and *PLATON* (Spek, 2020).

6. Refinement

Crystal data, data collection and structure refinement details are summarized in Table 3. All C-bound H atoms were positioned geometrically and refined using a riding model, with C—H = 0.95–1.00 Å and U_{iso}(H) = 1.2U_{eq}(C).

Acknowledgements

The authors' contributions are as follows; conceptualization MA and GMM; synthesis, VSM and VMC; X-ray analysis VNK; writing (review and editing of the manuscript) MA, KIH and NAG; supervision MA and GMM.

Funding information

Funding for this research was provided by: the RUDN University Scientific Projects Grant System (grant No. 021422-2-000), the Azerbaijan Medical University and Baku Engineering University.

References

Agilent (2014). *CrysAlis PRO*. Agilent Technologies Ltd, Yarnton, England.

Bernstein, J., Davis, R. E., Shimoni, L. & Chang, N.-L. (1995). *Angew. Chem. Int. Ed. Engl.* **34**, 1555–1573.

Clark, R. C. & Reid, J. S. (1995). *Acta Cryst.* A**51**, 887–897.

Cole, J. C. & Taylor, R. (2022). *Cryst. Growth Des.* **22**, 1352–1364.

Desiraju, G. R., Ho, P. S., Kloo, L., Legon, A. C., Marquardt, R., Metrangolo, P., Politzer, P., Resnati, G. & Rissanen, K. (2013). *Pure Appl. Chem.* **85**, 1711–1713.

Farrugia, L. J. (2012). *J. Appl. Cryst.* **45**, 849–854.

Groom, C. R., Bruno, I. J., Lightfoot, M. P. & Ward, S. C. (2016). *Acta Cryst.* B**72**, 171–179.

Guseinov, F. I., Samigullina, A. I., Hökelek, T., Hamidov, S. Z., Lasri, J., Hasanov, K. I., Javadzade, T. A. & Belay, A. N. (2025). *Acta Cryst.* E**81**, 672–675.

Huseynov, F. E., Mahmoudi, G., Hajiyeva, S. R., Shamilov, N. T., Zubkov, F. I., Nikitina, E. V., Prisyazhnyuk, E. D. & Kopylovich, M. N. (2021). *Polyhedron* **209**, 115453.

Javadzade, T. A., Hajiyeva, S. R., Chyragov, F. M., Nunes, A. V. M., Lasri, J., Hamidov, S. Z., Hasanov, K. I. & Mahmudov, K. T. (2026). *J. Organomet. Chem.* **1046**, 123901.

Macrae, C. F., Sovago, I., Cottrell, S. J., Galek, P. T. A., McCabe, P., Pidcock, E., Platings, M., Shields, G. P., Stevens, J. S., Towler, M. & Wood, P. A. (2020). *J. Appl. Cryst.* **53**, 226–235.

Makhmudova, N. I., Mammadov, E. S., Kerimli, F. S., Ilyasli, T. M., Akhmedova, N. F. & Mammadov, S. E. (2022). *Bull. Chem. React. Eng. Catal.* **17**, 725–732.

Mamedov, İ. G., Khrustalev, V. N., Akkurt, M., Kerimli, F. S., Bhattarai, A., Khalilov, A. N. & Naghiyev, F. N. (2024). *Acta Cryst.* E**80**, 495–500.

Maslova, V. S., Gomila, R. M., Dikusar, E. A., Zaytsev, V. P., Khrustalev, V. N., Zubkov, F. I. & Frontera, A. (2026). *J. Mol. Struct.* **1361**, 145700.

Mitchell, L. A., Stanley, J. M., Espinosa DeHoyos, L. & Holliday, B. J. (2013). *Acta Cryst.* C**69**, 638–641.

Politzer, P., Murray, J. S. & Clark, T. (2010). *Phys. Chem. Chem. Phys.* **12**, 7748–7757.

Reichenbächer, K., Süss, H. I. & Hulliger, J. (2005). *Chem. Soc. Rev.* **34**, 22–30.

Riley, K. E., Murray, J. S., Fanfrlík, J., Řezáč, J., Solá, R. J., Concha, M. C., Ramos, F. M. & Politzer, P. (2011). *J. Mol. Model.* **17**, 3309–3318.

Shchevnikov, D. M., Gurbanov, A. V., Khrustalev, V. N., Woldemariam, M. M., Hökelek, T. & Litvinov, R. A. (2026). *Acta Cryst.* E**82**, 572–577.

Sheldrick, G. M. (2015*a*). *Acta Cryst.* A**71**, 3–8.

Sheldrick, G. M. (2015*b*). *Acta Cryst.* C**71**, 3–8.

Spackman, P. R., Turner, M. J., McKinnon, J. J., Wolff, S. K., Grimwood, D. J., Jayatilaka, D. & Spackman, M. A. (2021). *J. Appl. Cryst.* **54**, 1006–1011.

Spek, A. L. (2020). *Acta Cryst.* E**76**, 1–11.

Tan, X.-J., Liu, S., Hei, X.-M., Yang, F.-C., He, P.-B., Guo, F. & Xing, D.-X. (2020). *Acta Cryst.* C**76**, 75–86.

Yang, F.-L., Yang, X., Wu, R.-Z., Yan, C.-X., Yang, F., Ye, W., Zhang, L.-W. & Zhou, P.-P. (2018). *Phys. Chem. Chem. Phys.* **20**, 11386–11395.

supporting information

Acta Cryst. (2026). E**82**, 1052-1056 [https://doi.org/10.1107/S2056989026008108]

Crystal structure and Hirshfeld surface analysis of 6-bromo-2-(pentafluorophenyl)-2,3,7,7a-tetrahydro-3a,6-epoxyisoindol-1(6*H*)-one

Viktoria S. Maslova, Veronika M. Cherepanova, Victor N. Khrustalev, Mehmet Akkurt, Gizachew Mulugeta Manahelohe, Khudayar I. Hasanov and Narmina A. Guliyeva

Computing details

6-Bromo-2-(pentafluorophenyl)-2,3,7,7a-tetrahydro-3a,6-epoxyisoindol-1(6*H*)-one

Crystal data

$C_{14}H_7BrF_5NO_2$
$M_r = 396.11$
Monoclinic, $P2_1/n$
$a = 13.4425$ (1) Å
$b = 7.0992$ (1) Å
$c = 14.9829$ (2) Å
$\beta = 106.241$ (1)°
$V = 1372.77$ (3) Å^3
$Z = 4$
$F(000) = 776$
$D_x = 1.917$ Mg m^{-3}
Cu $K\alpha$ radiation, $\lambda = 1.54184$ Å
Cell parameters from 10823 reflections
$\theta = 3.9$–$79.2°$
$\mu = 4.76$ mm^{-1}
$T = 100$ K
Prism, colourless
0.45 × 0.33 × 0.20 mm

Data collection

Rigaku XtaLAB Synergy-S, HyPix-6000HE area-detector diffractometer
Radiation source: micro-focus sealed X-ray tube
φ and ω scans
Absorption correction: analytical [CrysAlisPro (Agilent, 2014). Analytical numeric absorption correction using a multifaceted crystal model based on expressions derived by Clark & Reid (1995)]
$T_{min} = 0.385$, $T_{max} = 0.622$
15639 measured reflections
2965 independent reflections
2814 reflections with $I > 2\sigma(I)$
$R_{int} = 0.041$
$\theta_{max} = 79.7°$, $\theta_{min} = 3.9°$
$h = -17\rightarrow15$
$k = -8\rightarrow9$
$l = -19\rightarrow19$

Refinement

Refinement on F^2
Least-squares matrix: full
$R[F^2 > 2\sigma(F^2)] = 0.033$
$wR(F^2) = 0.094$
$S = 1.08$
2965 reflections
209 parameters
0 restraints
Primary atom site location: difference Fourier map
Secondary atom site location: difference Fourier map
Hydrogen site location: inferred from neighbouring sites
H-atom parameters constrained
$w = 1/[\sigma^2(F_o^2) + (0.0604P)^2 + 0.7868P]$ where $P = (F_o^2 + 2F_c^2)/3$
$(\Delta/\sigma)_{max} = 0.001$
$\Delta\rho_{max} = 0.56$ e Å^{-3}
$\Delta\rho_{min} = -0.65$ e Å^{-3}
Extinction correction: SHELXL-2019/2 (Sheldrick, 2015b), $Fc^*=kFc[1+0.001xFc^2\lambda^3/\sin(2\theta)]^{-1/4}$
Extinction coefficient: 0.00042 (4)

Special details

Geometry. All esds (except the esd in the dihedral angle between two l.s. planes) are estimated using the full covariance matrix. The cell esds are taken into account individually in the estimation of esds in distances, angles and torsion angles; correlations between esds in cell parameters are only used when they are defined by crystal symmetry. An approximate (isotropic) treatment of cell esds is used for estimating esds involving l.s. planes.

Fractional atomic coordinates and isotropic or equivalent isotropic displacement parameters (Å²)

	x	*y*	*z*	U_{iso}*/U_{eq}
Br1	0.71543 (2)	0.50666 (3)	0.31376 (2)	0.02411 (12)
F1	0.41520 (9)	0.89713 (18)	0.47110 (8)	0.0256 (3)
F2	0.31108 (11)	1.11945 (18)	0.56004 (9)	0.0331 (3)
F3	0.11978 (14)	1.01534 (19)	0.57004 (12)	0.0346 (4)
F4	0.03644 (10)	0.6834 (2)	0.49575 (11)	0.0366 (3)
F5	0.14074 (10)	0.45924 (19)	0.40680 (9)	0.0269 (3)
O1	0.31755 (10)	0.8046 (2)	0.27300 (9)	0.0210 (3)
C1	0.34540 (13)	0.6469 (3)	0.30167 (12)	0.0169 (3)
N2	0.33237 (12)	0.5708 (2)	0.38162 (11)	0.0173 (3)
C3	0.37373 (14)	0.3779 (3)	0.40281 (13)	0.0179 (4)
H3A	0.317546	0.282958	0.389051	0.021*
H3B	0.415050	0.365795	0.468547	0.021*
C3A	0.44098 (13)	0.3599 (3)	0.33735 (12)	0.0174 (3)
C4	0.46877 (15)	0.1797 (3)	0.29634 (14)	0.0225 (4)
H4	0.435122	0.061071	0.292247	0.027*
C5	0.55086 (15)	0.2237 (3)	0.26714 (14)	0.0231 (4)
H5	0.587321	0.143799	0.236301	0.028*
C6	0.57366 (14)	0.4291 (3)	0.29374 (13)	0.0192 (4)
C7	0.49343 (14)	0.5591 (3)	0.22739 (13)	0.0193 (4)
H7A	0.510124	0.694053	0.239826	0.023*
H7B	0.486588	0.530868	0.161231	0.023*
C7A	0.39609 (16)	0.5001 (2)	0.25605 (14)	0.0175 (4)
H7C	0.344171	0.437042	0.203514	0.021*
O8	0.54265 (9)	0.4439 (2)	0.37751 (9)	0.0176 (3)
C8	0.27993 (13)	0.6742 (3)	0.43498 (12)	0.0175 (4)
C9	0.32160 (14)	0.8430 (3)	0.47564 (13)	0.0202 (4)
C10	0.26888 (18)	0.9572 (3)	0.52161 (14)	0.0239 (4)
C11	0.17202 (16)	0.9045 (3)	0.52701 (14)	0.0249 (4)
C12	0.12954 (15)	0.7358 (3)	0.48870 (14)	0.0239 (4)
C13	0.18329 (14)	0.6216 (3)	0.44315 (13)	0.0200 (4)

Atomic displacement parameters (Å²)

	U^{11}	U^{22}	U^{33}	U^{12}	U^{13}	U^{23}
Br1	0.01600 (16)	0.02940 (18)	0.02836 (17)	−0.00105 (6)	0.00857 (11)	−0.00042 (7)
F1	0.0191 (5)	0.0281 (6)	0.0304 (6)	−0.0076 (4)	0.0084 (4)	−0.0045 (5)
F2	0.0456 (8)	0.0238 (6)	0.0326 (6)	−0.0059 (6)	0.0155 (6)	−0.0088 (5)
F3	0.0433 (9)	0.0313 (7)	0.0382 (8)	0.0107 (5)	0.0261 (7)	−0.0001 (5)
F4	0.0260 (6)	0.0386 (8)	0.0543 (8)	−0.0011 (5)	0.0262 (6)	0.0023 (6)

F5	0.0237 (6)	0.0256 (6)	0.0341 (7)	−0.0083 (5)	0.0126 (5)	−0.0035 (5)
O1	0.0180 (6)	0.0217 (7)	0.0235 (6)	0.0021 (5)	0.0064 (5)	0.0053 (5)
C1	0.0131 (7)	0.0196 (9)	0.0175 (8)	−0.0031 (6)	0.0036 (6)	0.0004 (6)
N2	0.0156 (7)	0.0181 (8)	0.0188 (7)	0.0011 (6)	0.0059 (6)	0.0015 (6)
C3	0.0189 (8)	0.0161 (9)	0.0195 (8)	0.0004 (7)	0.0068 (7)	0.0018 (6)
C3A	0.0156 (8)	0.0183 (8)	0.0182 (8)	−0.0019 (6)	0.0046 (6)	−0.0004 (6)
C4	0.0248 (9)	0.0169 (9)	0.0262 (9)	0.0000 (7)	0.0078 (7)	−0.0024 (7)
C5	0.0246 (9)	0.0204 (9)	0.0255 (9)	0.0026 (7)	0.0089 (7)	−0.0028 (7)
C6	0.0159 (8)	0.0214 (10)	0.0219 (9)	0.0001 (7)	0.0082 (7)	−0.0006 (7)
C7	0.0160 (8)	0.0234 (9)	0.0191 (8)	0.0003 (7)	0.0061 (7)	0.0030 (7)
C7A	0.0175 (10)	0.0187 (10)	0.0163 (9)	−0.0009 (6)	0.0046 (7)	0.0010 (6)
O8	0.0143 (6)	0.0205 (6)	0.0180 (6)	−0.0020 (5)	0.0047 (5)	−0.0008 (5)
C8	0.0159 (8)	0.0194 (9)	0.0173 (8)	0.0013 (6)	0.0046 (6)	0.0022 (7)
C9	0.0173 (8)	0.0224 (9)	0.0208 (8)	−0.0028 (7)	0.0053 (7)	0.0009 (7)
C10	0.0315 (11)	0.0187 (9)	0.0221 (9)	−0.0013 (8)	0.0084 (8)	−0.0021 (8)
C11	0.0291 (10)	0.0261 (10)	0.0236 (9)	0.0079 (8)	0.0144 (8)	0.0031 (8)
C12	0.0200 (8)	0.0270 (10)	0.0282 (9)	0.0020 (7)	0.0124 (7)	0.0053 (8)
C13	0.0184 (8)	0.0216 (9)	0.0204 (8)	−0.0018 (7)	0.0061 (7)	0.0017 (7)

Geometric parameters (Å, º)

Br1—C6	1.9249 (18)	C4—C5	1.333 (3)
F1—C9	1.335 (2)	C4—H4	0.9500
F2—C10	1.341 (2)	C5—C6	1.520 (3)
F3—C11	1.335 (2)	C5—H5	0.9500
F4—C12	1.338 (2)	C6—O8	1.433 (2)
F5—C13	1.334 (2)	C6—C7	1.550 (3)
O1—C1	1.220 (2)	C7—C7A	1.545 (3)
C1—N2	1.369 (2)	C7—H7A	0.9900
C1—C7A	1.509 (3)	C7—H7B	0.9900
N2—C8	1.411 (2)	C7A—H7C	1.0000
N2—C3	1.479 (2)	C8—C13	1.389 (3)
C3—C3A	1.514 (2)	C8—C9	1.389 (3)
C3—H3A	0.9900	C9—C10	1.381 (3)
C3—H3B	0.9900	C10—C11	1.379 (3)
C3A—O8	1.458 (2)	C11—C12	1.381 (3)
C3A—C4	1.511 (3)	C12—C13	1.386 (3)
C3A—C7A	1.558 (3)		

O1—C1—N2	124.63 (17)	C7A—C7—H7A	112.0
O1—C1—C7A	127.38 (16)	C6—C7—H7A	112.0
N2—C1—C7A	107.96 (15)	C7A—C7—H7B	112.0
C1—N2—C8	119.81 (16)	C6—C7—H7B	112.0
C1—N2—C3	114.88 (15)	H7A—C7—H7B	109.7
C8—N2—C3	125.28 (15)	C1—C7A—C7	117.64 (15)
N2—C3—C3A	101.29 (14)	C1—C7A—C3A	102.24 (15)
N2—C3—H3A	111.5	C7—C7A—C3A	102.56 (15)
C3A—C3—H3A	111.5	C1—C7A—H7C	111.2

N2—C3—H3B	111.5	C7—C7A—H7C	111.2
C3A—C3—H3B	111.5	C3A—C7A—H7C	111.2
H3A—C3—H3B	109.3	C6—O8—C3A	94.44 (13)
O8—C3A—C4	101.77 (14)	C13—C8—C9	117.71 (17)
O8—C3A—C3	111.03 (14)	C13—C8—N2	122.55 (17)
C4—C3A—C3	126.55 (16)	C9—C8—N2	119.55 (16)
O8—C3A—C7A	100.07 (14)	F1—C9—C10	118.60 (18)
C4—C3A—C7A	107.98 (15)	F1—C9—C8	119.73 (17)
C3—C3A—C7A	106.37 (15)	C10—C9—C8	121.67 (18)
C5—C4—C3A	104.88 (17)	F2—C10—C11	120.07 (19)
C5—C4—H4	127.6	F2—C10—C9	120.28 (19)
C3A—C4—H4	127.6	C11—C10—C9	119.7 (2)
C4—C5—C6	105.28 (16)	F3—C11—C10	120.1 (2)
C4—C5—H5	127.4	F3—C11—C12	119.99 (19)
C6—C5—H5	127.4	C10—C11—C12	119.90 (18)
O8—C6—C5	102.30 (15)	F4—C12—C11	119.69 (18)
O8—C6—C7	101.40 (14)	F4—C12—C13	120.31 (19)
C5—C6—C7	110.46 (15)	C11—C12—C13	120.00 (18)
O8—C6—Br1	111.13 (12)	F5—C13—C12	118.90 (17)
C5—C6—Br1	115.69 (13)	F5—C13—C8	120.05 (17)
C7—C6—Br1	114.25 (13)	C12—C13—C8	121.04 (18)
C7A—C7—C6	98.75 (14)		

O1—C1—N2—C8	2.6 (3)	Br1—C6—O8—C3A	−174.99 (12)
C7A—C1—N2—C8	−175.69 (15)	C4—C3A—O8—C6	52.09 (16)
O1—C1—N2—C3	−179.22 (16)	C3—C3A—O8—C6	−170.87 (15)
C7A—C1—N2—C3	2.5 (2)	C7A—C3A—O8—C6	−58.85 (15)
C1—N2—C3—C3A	14.4 (2)	C1—N2—C8—C13	111.4 (2)
C8—N2—C3—C3A	−167.53 (16)	C3—N2—C8—C13	−66.6 (2)
N2—C3—C3A—O8	83.26 (17)	C1—N2—C8—C9	−63.5 (2)
N2—C3—C3A—C4	−152.88 (17)	C3—N2—C8—C9	118.5 (2)
N2—C3—C3A—C7A	−24.69 (18)	C13—C8—C9—F1	178.66 (16)
O8—C3A—C4—C5	−34.54 (19)	N2—C8—C9—F1	−6.2 (3)
C3—C3A—C4—C5	−162.19 (18)	C13—C8—C9—C10	−0.9 (3)
C7A—C3A—C4—C5	70.3 (2)	N2—C8—C9—C10	174.27 (18)
C3A—C4—C5—C6	1.7 (2)	F1—C9—C10—F2	0.5 (3)
C4—C5—C6—O8	32.27 (19)	C8—C9—C10—F2	−179.92 (18)
C4—C5—C6—C7	−75.0 (2)	F1—C9—C10—C11	179.84 (17)
C4—C5—C6—Br1	153.23 (14)	C8—C9—C10—C11	−0.6 (3)
O8—C6—C7—C7A	−41.07 (17)	F2—C10—C11—F3	0.4 (3)
C5—C6—C7—C7A	66.82 (18)	C9—C10—C11—F3	−178.97 (19)
Br1—C6—C7—C7A	−160.68 (12)	F2—C10—C11—C12	−178.90 (19)
O1—C1—C7A—C7	52.6 (3)	C9—C10—C11—C12	1.8 (3)
N2—C1—C7A—C7	−129.20 (17)	F3—C11—C12—F4	−0.6 (3)
O1—C1—C7A—C3A	163.98 (17)	C10—C11—C12—F4	178.65 (19)
N2—C1—C7A—C3A	−17.80 (19)	F3—C11—C12—C13	179.31 (18)
C6—C7—C7A—C1	115.08 (18)	C10—C11—C12—C13	−1.4 (3)
C6—C7—C7A—C3A	3.86 (17)	F4—C12—C13—F5	−0.1 (3)

O8—C3A—C7A—C1	−89.03 (15)	C11—C12—C13—F5	179.93 (17)
C4—C3A—C7A—C1	164.97 (15)	F4—C12—C13—C8	179.81 (17)
C3—C3A—C7A—C1	26.57 (18)	C11—C12—C13—C8	−0.1 (3)
O8—C3A—C7A—C7	33.29 (17)	C9—C8—C13—F5	−178.79 (17)
C4—C3A—C7A—C7	−72.70 (18)	N2—C8—C13—F5	6.2 (3)
C3—C3A—C7A—C7	148.89 (15)	C9—C8—C13—C12	1.3 (3)
C5—C6—O8—C3A	−50.93 (15)	N2—C8—C13—C12	−173.77 (17)
C7—C6—O8—C3A	63.21 (15)		

Hydrogen-bond geometry (Å, º)

Cg5 is the centroid of the pentafluorophenyl ring (C8–C13).

D—H···*A*	*D*—H	H···*A*	*D*···*A*	*D*—H···*A*
C3—H3*A*···O1^{i}	0.99	2.60	3.167 (2)	117
C3—H3*B*···O8^{ii}	0.99	2.60	3.410 (2)	140
C4—H4···O1^{iii}	0.95	2.38	3.309 (3)	167
C7*A*—H7*C*···O1^{i}	1.00	2.48	3.109 (3)	120
C7*A*—H7*C*···*Cg*5^{i}	1.00	2.87	3.790 (2)	153

Symmetry codes: (i) −*x*+1/2, *y*−1/2, −*z*+1/2; (ii) −*x*+1, −*y*+1, −*z*+1; (iii) *x*, *y*−1, *z*.